JGR Oceans

RESEARCH ARTICLE

10.1029/2024JC021415

Critical Times for the Critical Depth Theory

Žarko Kovač[1] and **Shubha Sathyendranath**[2]

[1]Faculty of Science, University of Split, Split, Croatia, [2]National Centre for Earth Observations, Plymouth Marine Laboratory, Plymouth, UK

Key Points:

- Interaction of phytoplankton with the underwater light field sets up a bio-optical feedback mechanism creating constants of motion
- A new differential equation shows that the light intensities at both the compensation depth and the critical depth are constants of motion
- Mixed-layer depth acts as the bifurcation parameter, and the critical depth is identified as the bifurcation point

Correspondence to:

Ž. Kovač,
zkovac@pmfst.hr

Citation:

Kovač, Ž., & Sathyendranath, S. (2025). Critical times for the critical depth theory. *Journal of Geophysical Research: Oceans*, *130*, e2024JC021415. https://doi.org/10.1029/2024JC021415

Received 1 JUN 2024
Accepted 1 APR 2025

Author Contributions:

Conceptualization: Žarko Kovač
Formal analysis: Žarko Kovač, Shubha Sathyendranath
Funding acquisition: Žarko Kovač, Shubha Sathyendranath
Investigation: Žarko Kovač, Shubha Sathyendranath
Methodology: Žarko Kovač, Shubha Sathyendranath
Project administration: Žarko Kovač, Shubha Sathyendranath
Visualization: Žarko Kovač
Writing – original draft: Žarko Kovač
Writing – review & editing: Žarko Kovač, Shubha Sathyendranath

Abstract

Critical Depth Hypothesis is arguably one of the longest standing biophysical theories in oceanography and is the earliest mathematically formulated theory aimed at explaining the phenomenon of phytoplankton blooms. It introduces a depth horizon, termed the critical depth, at which the integrated primary production from the surface to that depth equals the integrated loss terms within the same layer. In mixed layers deeper than the critical depth, losses dominate photosynthesis and vice versa. A related horizon in case of week mixing is the compensation depth, where the rate of photosynthesis matches the loss rate. In this paper, the effect of phytoplankton light attenuation on the critical depth is examined, showing that it creates a bio-optical feedback in the model. A new differential equation, derived for the time evolution of the compensation depth reveals that the light intensities at both the compensation depth and the critical depth are constants of motion. Exact solutions for average and total mixed layer biomass at steady state are derived, and their stability properties are analyzed. An existence of a bio-optical bifurcation is shown, in which the mixed layer depth acts as the bifurcation parameter and the critical depth is identified as the bifurcation point. Transients between steady states are also explored, and it is shown that the relation between the initial condition and the final steady state is paramount in determining whether a shallowing or deepening of the mixed layer will lead to a rise or a decline in biomass over time.

Plain Language Summary

The Critical Depth Hypothesis attempts to explain why and how phytoplankton blooms occur. The theory introduces the concept of a critical depth, which is the depth at which the total production of phytoplankton from the surface down to it equals the total losses. If the ocean's mixed layer is deeper than this critical depth, the average light level is too low for photosynthesis to keep up with losses. In areas of the ocean with weak mixing, there is a related concept called the compensation depth, where the rate of photosynthesis exactly matches the loss rate at depth. This paper explores how phytoplankton's light absorption affects its critical and compensation depths, creating a feedback loop. A new equation shows that light levels at both the compensation and critical depths remain constant over time. The study also provides exact solutions for the amount of phytoplankton in the mixed layer when the system is at steady state and also demonstrates that the system can have a stable and an unstable steady state. It is shown that the stability of the system is determined by how deep the mixed layer is in comparison to the critical depth.

1. Introduction

The pelagic ecosystem is an open, dissipative system that requires a steady supply of external energy (sunlight) and matter (nutrients) to maintain it (Platt et al., 1984). As sunlight penetrates through the ocean surface, most of its energy serves to heat the ocean. A portion of the photons, albeit small in absolute terms, ends up being used to drive photosynthesises, which in the ocean is predominantly carried out by phytoplankton, the ocean's free-floating autotrophs (Williams & Follows, 2011). In photosynthesis, inorganic carbon gets assimilated and converted to organic matter and the process is termed primary production in ecology (Regaudie-de Gioux et al., 2014). The energy stored in the newly formed organic matter is not only used by phytoplankton but is also an energy source to fuel the rest of the ecosystem via trophic transfer (Duarte et al., 2013).

Global marine primary production is comparable to its terrestrial counterpart at the annual timescale (Field et al., 1998), jointly totalling at around 100 gigatons per annum (Raven & Falkowski, 1999). It is precisely at the global scale, where due to remote sensing technologies and state-of-the-art models, which have been long in the making (Longhurst et al., 1995; Platt & Sathyendranath, 1988), that our ability to calculate primary production has reached highly advanced technical levels (Kulk et al., 2020, 2021). These advances in remote sensing have paralleled great strides in large-scale models of the marine ecosystem, within which primary production models of varying degrees of complexity play a central role (Laufkötter et al., 2013).

Nevertheless, there are unresolved questions: satellite-based primary production models agree reasonably well with each other at the global scale, converging to a value of around 50 gigatons per annum (Kulk et al., 2020, 2021; Sathyendranath et al., 2020), but there is less agreement on the magnitude and sign of the global trends seen in satellite data (Westberry et al., 2023). There is also a high level of uncertainty in the future primary production values and trends estimated from ecosystem models (Laufkötter et al., 2015).

In comparison to the global scale, at smaller spatial, and shorter temporal, scales, our ability to predict primary production is arguably less satisfactory. The reason for this may be, and often is, attributed to the underlying complexities of the marine ecosystem, with far too many state variables to estimate correctly the initial conditions and the sensitivity of the dynamics of both the ecosystem (Cropp et al., 2014; Huisman et al., 2006) and the physical environment (Mann & Lazier, 2005) to the initial conditions. These are the two ingredients, which render prediction hard from a dynamical systems point of view (Strogatz, 2015). Therefore, even under the prevalent assumption that the governing equations describing the temporal evolution of marine ecosystems are precise descriptions of the intricate processes involved, there is still a limit on the predictive ability of models (Huisman & Weissing, 2001), a standard trademark of chaotic systems (Ott, 2002).

Consequently, and despite the confidence in the exactness of model formulations, there is considerable debate in the biophysical oceanographic community as to what is the dominant underlying mechanism governing the temporal and spatial evolution of phytoplankton biomass and subsequently the carbon flux associated with primary production. This is strongly evident in recent debates found in the literature on ocean blooms, such as Chiswell (2011), Behrenfeld et al. (2013a), Chiswell (2013), and Behrenfeld et al. (2013b). In many of these studies, the crux of the discussion evolves around the mechanism for initiating phytoplankton blooms, as it is here that quantitative and even qualitative features of models are put to the test. The discussion on phytoplankton responses to external forcing is also relevant for addressing questions related to resilience and stability of phytoplankton and primary production (Kovač et al., 2020) in a changing climate (Rocha, 2022), and when investigating questions related to potential abrupt changes or tipping points in the Earth's biosphere (Lenton et al., 2022).

In this context, theoretical investigations provide additional and complementary information on the interplay between primary production and the factors that control it and on feedbacks between them. Historically, the Critical Depth Hypothesis has provided a strong theoretical framework on which to explore the biophysical mechanism of phytoplankton blooms (Sathyendranath et al., 2015) is explored. It traces its origins back to the ideas of Gran and Braarud (1935), with the mathematical formulation first laid out by Sverdrup (1953). The hypothesis postulates that a bloom is initiated once the mixed layer becomes shallower than the critical depth: a depth horizon above which integrated production is higher than all the losses, hence the name. The process of mixed-layer shallowing typically occurs in spring, with the onset of stratification due to the increase in solar heating and abatement of winter storms. Because in the midlatitudes blooms naturally take place in spring, it was viewed as a good explanation of the bloom onset mechanism for quite some time, with Sverdrup's (1953) paper coming to prominence in biophysical oceanography (Sathyendranath et al., 2015).

The Critical Depth Hypothesis is but one of a few candidate theories aimed at explaining phytoplankton blooms (Chiswell et al., 2015). Other theories rivalling it, or better to say complementing it, are the Critical Light Hypothesis by Huisman and Weissing (1994), the Critical Turbulence Hypothesis, by Huisman et al. (1999a), and the Dilution Recoupling Hypothesis by Behrenfeld (2010). All the mentioned theories are based on well-established physical laws, such as conservation of mass and energy, along with well-established biophysical parametrizations, at the center of which is the response of primary production to light (Jassby & Platt, 1976; Kovač et al., 2017). However, despite being based on the advection-diffusion-reaction equation describing the biomass distribution of phytoplankton (Ryabov & Blasius, 2008), these hypotheses differ in the identification of the mechanism responsible for bloom initiation in the ocean. The structure of the mathematical models allows for different dynamics to occur under different conditions, as evident and as correctly identified by the aforementioned authors. From this perspective, the hypotheses are not mutually exclusive, but rather complement each other. The divergence in the literature emerges at the stage of determining which mechanism predominates in the ocean.

The Critical Light Hypothesis due to Huisman and Weissing (1994) states that it is not the critical depth which is relevant, but the critical light one would measure at the bottom of a mixed layer once a monoculture population acquires a steady state. Another insight from the same authors is the Critical Turbulence Hypothesis (Huisman et al., 1999a). Here, a mechanism for bloom initiation is revealed in the absence of strong mixing, enabling phytoplankton to accumulate near the surface. Finally, the Dilution Recoupling Hypothesis (Behrenfeld, 2010), suggests that biomass accumulation can occur once the grazing pressure from zooplankton declines, due to a reduction in phytoplankton-zooplankton encounter rates. This typically occurs in autumn with storms initiating strong mixing. The hypothesis makes the opposite prediction to Sverdrup's, in that it suggests that blooms can occur when mixed-layer depth increases.

Recently it was shown by Kovač et al. (2021) that the Critical Depth Hypothesis (Sverdrup, 1953) and the Critical Light Hypothesis (Huisman & Weissing, 1994) can in fact be unified mathematically under a conservation principle. The principle in question relies on the bio-optical feedback mechanism, which occurs due to the interaction of phytoplankton with the underwater light field, with phytoplankton close to the surface shading phytoplankton below them, forcing the system toward a steady state. Such a feedback process is normally included in all phytoplankton models, be they analytical or numerical, but very few authors have paid grave attention to its consequences, apart from Platt, Sathyendranath, et al. (2003) and Edwards et al. (2004), among others. In this paper, we demonstrate how the dynamical coupling of phytoplankton to the underwater light field is central to the issue of bloom formation, and leads to unification of apparently divergent theories regarding the underlying mechanisms. The combination of the concept of critical depth with the theory of dynamical systems leads to new insights into system stability and transients, in which bio-optical coupling plays a key role.

2. Mathematical Model

Let the z axis be positive downward, with the origin at the sea surface. Let B stand for phytoplankton biomass, here expressed as chlorophyll concentration, such that at any given time, $B(z,t)$ gives the biomass at depth, with the description of biomass as a function of depth being termed the biomass profile. In the ocean, the biomass profile is shaped by photosynthesis, losses, sinking, and mixing (Huisman et al., 2002). In generic dynamical models of the biomass profile, these processes are usually encompassed in a differential equation for B written as

$$\frac{\partial B}{\partial t} = \left(P^B - L^B\right) B - \frac{\partial F}{\partial z}, \tag{1}$$

where P^B stands for photosynthesis and L^B for losses, both per unit biomass, and F is the flux, with contributions from sinking and mixing, which can be expressed as

$$F = wB - M\frac{\partial B}{\partial z}, \tag{2}$$

where w is the sinking speed and M is the mixing coefficient (Huisman & Sommeijer, 2002b). In general, all parameters in the model can be depth- and time-dependent.

The photosynthesis term P^B gets its depth and time dependence due to irradiance I (Platt & Sathyendranath, 1991). Photosynthesis also depends on nutrients, but the focus of this paper is on light dependence; therefore, nutrient limitation of photosynthesis is not considered. The photosynthesis-light relation is specified with the following photosynthesis irradiance function:

$$P^B(z,t) = p^B(I(z,t)), \tag{3}$$

which is a nonlinear function representing the photophysiological coupling of chlorophyll to the rate of carbon assimilation in photosynthesis, termed primary production in ecology (Kovač et al., 2017). For brevity, we refer to P^B as the production term.

Irradiance gets attenuated with depth due to absorption and scattering of light by seawater and phytoplankton (Kirk, 2011). When using the wording seawater, we implicitly assume all constituents which attenuate light that are not associated with phytoplankton, such as water itself, allochthonous colored dissolved organic matter, and particles. On the other hand, attenuation by substances that covary with phytoplankton (such as autochthonous colored dissolved organic matter, and other biological particles) can be included in the phytoplankton term. We then model the effect of phytoplankton on irradiance using the Beer-Lambert law as follows:

$$\frac{\mathrm{d}I}{\mathrm{d}z} = -(K_w + k_B B)\, I, \tag{4}$$

where K_w is the diffuse attenuation coefficient of downwelling light associated with seawater and k_B is the specific attenuation coefficient of phytoplankton and covarying substances (Platt, Sathyendranath, et al., 2003). Note that K_w could, in principle, include attenuation by any other substance that, along with water, may contribute to a constant background attenuation. With this equation, a bio-optical feedback is set up: biomass distribution affects the underwater light field, which affects primary production and this feeds back to shape the biomass profile (Shigesada & Okubo, 1981). At any given time, irradiance at depth is given by the vertical integral of the above expression:

$$I(z,t) = I_0(t) \exp\left[-\int_0^z (K_w + k_B B(z',t))\, \mathrm{d}z' \right], \tag{5}$$

where $I_0(t)$ is surface irradiance and z' is a dummy variable for integration. For the remainder of the paper, we assume constant surface irradiance $I_0(t) = I_0$.

3. Bio-Optical Constants of Motion

As stated in (5), irradiance is calculated at depth as a function of time. An alternative view would be to look at a predefined irradiance value and observe how it changes with depth over time, as a consequence of biological and physical processes. Of particular interest is the compensation irradiance I_c, which is the irradiance at which production matches losses (Huisman et al., 1999b):

$$p^B(I_c) = L^B. \tag{6}$$

Due to light attenuation, irradiance declines with depth (5) and so does production (Kovač, Platt, Sathyendranath, et al., 2016). Assuming production per unit biomass at the surface is larger than losses $P^B(0,t) > L^B$, which we have to assume to obtain positive solutions; there will be a depth at which production will equal losses, termed the compensation depth z_c (Sverdrup, 1953) (Figure 1):

$$P^B(z_c) = L^B. \tag{7}$$

At this depth, irradiance will equal the compensation irradiance $I(z_c,t) = I_c$. Complementarily, from Equation (5), irradiance at the compensation depth equals:

$$I(z_c) = I_0 \exp\left[-\int_0^{z_c} (K_w + k_B B(z,t))\, \mathrm{d}z \right]. \tag{8}$$

By definition, production at the compensation depth equals losses. Given that production is determined only by irradiance in model (3) implies that irradiance at the compensation depth cannot change over time, but the compensation depth z_c can, such that $I(z_c(t)) = I_c$ and $z_c = z_c(t)$, while keeping the irradiance at the compensation depth constant. Mathematically, the term inside the brackets in Equation (8) is conserved over time:

$$\frac{\mathrm{d}}{\mathrm{d}t}\left[K_w z_c(t) + k_B \int_0^{z_c(t)} B(z,t)\mathrm{d}z \right] = 0. \tag{9}$$

where integration over depth was carried out from zero to z_c. Rearranging terms yields an equation for the time evolution of the compensation depth as follows:

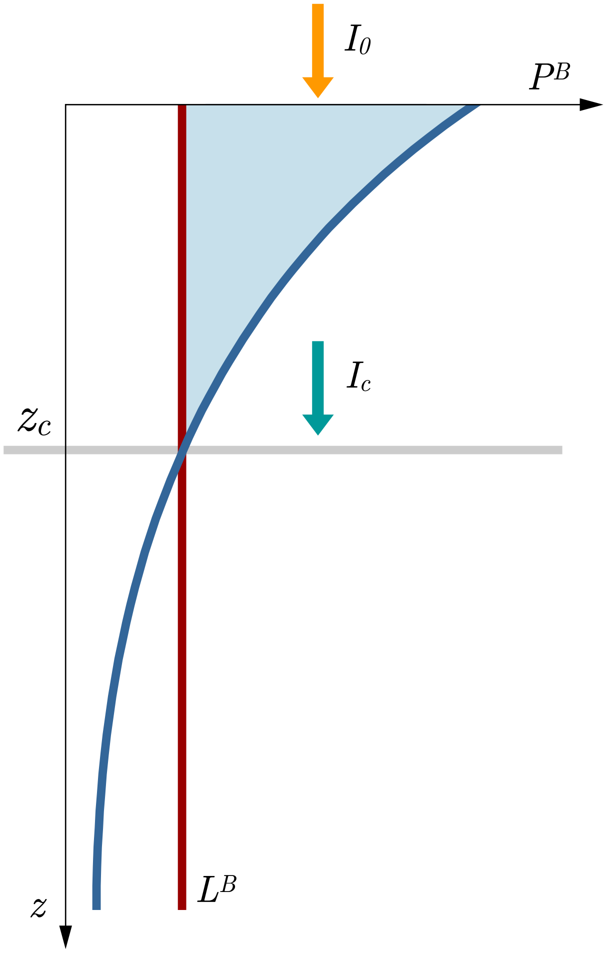

Figure 1. Due to the attenuation of light, photosynthesis P^B (blue curve) declines with depth and has to at some depth equal the loss rate L^B (red line). This depth is called the compensation depth z_c (gray line). Irradiance at the surface is given by I_0 (orange arrow) and irradiance at the compensation depth by I_c (green arrow).

$$\frac{\mathrm{d}z_c(t)}{\mathrm{d}t} = -\frac{k_B}{K_w + k_B B(z_c(t))} \int_0^{z_c(t)} \frac{\mathrm{d}B(z,t)}{\mathrm{d}t}\mathrm{d}z, \tag{10}$$

where the Leibnitz integral rule was applied. We observe that as the biomass above the compensation depth grows, the compensation depth becomes shallower, and vice versa. The system does so while keeping condition (9) satisfied, implying $K_w z_c(t) + k_B \int_0^{z_c(t)} B(z,t)\mathrm{d}z$ is a constant of motion. Following Equation (8), we can restate this condition as follows:

$$\frac{\mathrm{d}}{\mathrm{d}t} I(z_c(t)) = 0. \tag{11}$$

Of primary interest in this paper is the behavior of the system under strong mixing. A prototypical model in this case is that of a well-mixed upper ocean layer, with active mixing keeping the biomass uniform from the surface to the mixed-layer base Z_m. The model for the time evolution of mixed-layer biomass is obtained from Equation (1) by vertical integration from the surface to the mixed-layer base (Kovač et al., 2021), under no flux boundary conditions, to obtain the following:

$$\frac{\mathrm{d}B}{\mathrm{d}t} = \frac{1}{Z_m} \int_0^{Z_m} B p^B(I)\mathrm{d}z - L^B B, \tag{12}$$

where due to strong mixing, the biomass term is uniform with depth. We can now easily calculate the evolution of the compensation depth by applying (Equation 10) as follows:

$$\frac{\mathrm{d}z_c}{\mathrm{d}t} = -\left(\frac{k_B}{K_w + k_B B} \frac{\mathrm{d}B}{\mathrm{d}t}\right) z_c \tag{13}$$

where biomass is taken out of the integral over depth. The derived equation describes the temporal evolution of the compensation depth for the case of strong mixing. Using this solution, we can explore whether the compensation depth can reach a steady state z_c^*, where * marks steady state, mathematically stated as

$$\left.\frac{\mathrm{d}z_c}{\mathrm{d}t}\right|_{z_c^*} = 0. \tag{14}$$

Under steady state, the $\mathrm{d}B/\mathrm{d}t$ term in Equations (12) and (13) equals zero. From Equation (12), at steady state, we have a balance between production and losses in the mixed layer:

$$\int_0^{Z_m} p^B(I)\mathrm{d}z = L^B Z_m, \tag{15}$$

which is only possible if:

$$z_c < Z_m. \tag{16}$$

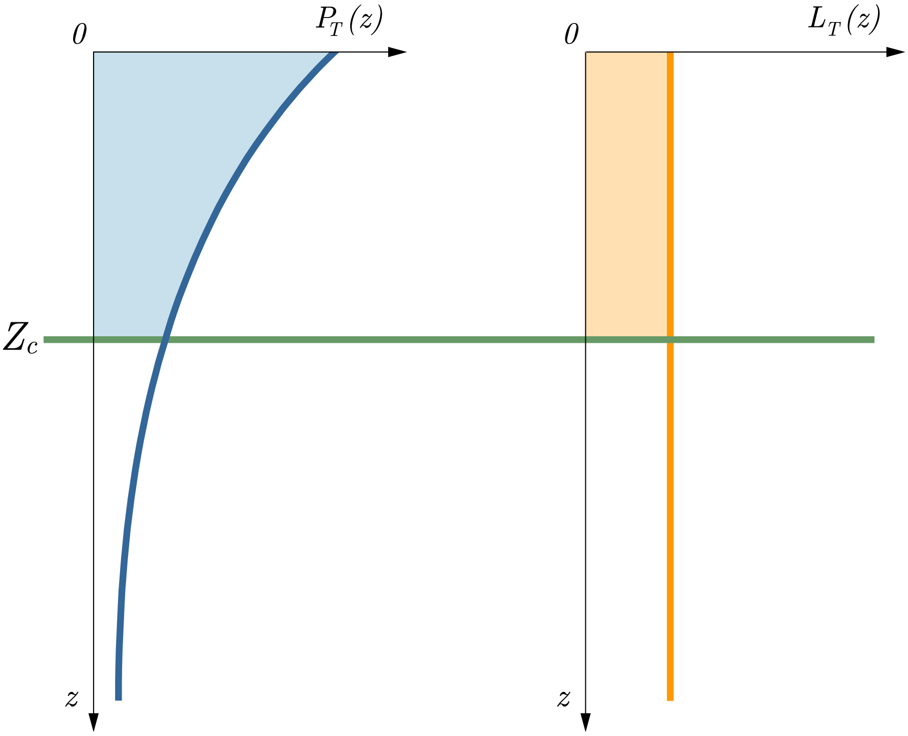

Figure 2. Graphical representation of the critical depth Z_c (green line) as the depth at which vertically integrated production (blue surface) equals vertically integrated losses (orange surface) in the mixed layer. When the mixed layer is shallower than the critical depth, production outweighs losses, which favors growth. When the mixed layer is deeper than the critical depth, losses outweigh production, which does not favor growth.

To demonstrate the validity of this condition, following Huisman and Weissing (1994), we set (Equation 12) equal to zero and partition the integral on the right-hand side of Equation (12) as

$$\int_0^{z_c} p^B(I)\mathrm{d}z - L^B z_c = -\int_{z_c}^{Z_m} p^B(I)\mathrm{d}z + L^B(Z_m - z_c). \tag{17}$$

The left-hand side is positive, given that by definition production is higher than losses above the compensation depth, and hence, when depth integration of the production term is carried out from the surface to the compensation depth, it is higher than the loss term integrated over the same depth range, making the left-hand side positive. To match the left-hand side, the right-hand side also has to be positive and for this to hold, the integral on the right-hand side has to be less than the loss term on the right-hand side. Because the production profile is a decreasing function of depth (Kovač, Platt, Morović, & Morović, 2016), for this to hold, the compensation depth has to be shallower than the mixed-layer depth to allow production to be less than the loss rate below z_c and up to Z_m. This is precisely what condition (Equation 16) states.

Condition (Equation 16) has one subtle consequence that has perhaps not been recognized earlier in the literature. Namely, it implies that the light intensity at the base of the mixed layer at steady state is lower than the critical light intensity I_c. This further implies that the loss term dominates over the production term below the mixed layer $(z > Z_m)$ under steady state as follows:

$$P^B(z) < L^B. \tag{18}$$

Subsequently, biomass cannot be sustained below the mixed layer, formally justifying the common assumption in mixed-layer production models: that growth is unfavorable below the mixed layer. According to the analysis presented here, it is no longer an assumption, but a consequence of the bio-optical feedback in the mixed layer.

Apart from the compensation depth, another depth horizon that is important for analyzing mixed-layer dynamics is the critical depth (Platt et al., 1991; Sverdrup, 1953). Critical depth Z_c (Figure 2) is defined as the depth at which mixed layer production equals mixed layer losses:

$$\int_0^{Z_c} p^B(I)\mathrm{d}z = L^B Z_c. \tag{19}$$

Comparison with Equation (15) shows that at steady state $Z_c = Z_m$, a result which was derived first by Platt, Broomhead, et al. (2003). However, if at any particular time $Z_c \neq Z_m$ a dynamical response follows and biomass either grows over time, for the case when the mixed layer is shallower than the critical depth, or declines over time, for the case when the mixed layer is deeper than the critical depth. This behavior is well established in the literature and forms the backbone of the Critical Depth Hypothesis (Sathyendranath et al., 2015).

What is less well known is how the critical depth evolves over time and it was only recently shown by Kovač et al. (2021) for the model of Sverdrup (1953) that:

$$\frac{\mathrm{d}Z_c}{\mathrm{d}t} = -\left(\frac{k_B}{K_w + k_B B}\frac{\mathrm{d}B}{\mathrm{d}t}\right)Z_c. \tag{20}$$

Interestingly, this equation is of the same form as Equation 13 derived here, which is in fact the statement of the Critical Depth Conservation Principle (Kovač et al., 2021). The principle states that the product of the diffuse attenuation coefficient for downwelling light, for the mixed layer, and the critical depth itself, is a constant of motion, mathematically stated as

$$\frac{\mathrm{d}}{\mathrm{d}t}(K_w + k_B B)Z_c = 0. \tag{21}$$

Because the light intensity at the critical depth Z_c is:

$$I(Z_c) = I_0 \exp(-(K_w + k_B B)Z_c), \tag{22}$$

it follows from Equation (21) that $I(Z_c)$ does not change with time. Therefore, mixed layer biomass evolves over time keeping the light intensity at the critical depth constant as follows:

$$\frac{\mathrm{d}}{\mathrm{d}t}I(Z_c(t)) = 0. \tag{23}$$

Therefore, both the light intensity at the compensation depth (Equation 11) and the light intensity at the critical depth (Equation 23) are constants of motion. The fact that only biomass enters both Equations (10) and (20) implies that these expressions are independent of the actual form of the photosynthesis irradiance function that is used in the biomass growth equation. The exact form of the photosynthesis irradiance function sets the quantitative dynamics of biomass, but does not affect the validity of the conservation principle.

4. Steady State

Given the assumption that mixing is faster than the growth rate, biomass is uniform in the mixed layer. Therefore, total biomass in the mixed layer at any time, labelled B_Z, is given by:

$$B_Z = BZ_m. \tag{24}$$

From here on we will refer to B as average biomass and B_Z as total biomass. A detailed discussion on the relation between B and B_Z is found in Behrenfeld and Boss (2014) and Freilich et al. (2021). As demonstrated in the prior section, time evolution of average biomass is given by Equation (12). By acknowledging (Equation 24), this equation is easily rewritten as:

$$\frac{\mathrm{d}B_Z}{\mathrm{d}t} = \int_0^{Z_m} Bp^B(I)\mathrm{d}z - L^B B_Z. \tag{25}$$

Note the difference in the production terms between the equations for total (Equation 25) and average biomass (Equation 12). In the equation for average biomass, the production term is divided by Z_m, whereas in the equation for total biomass, it is not. However, for a time-independent mixed-layer depth $Z_m \neq Z_m(t)$ and time-independent surface irradiance $I_0 \neq I_0(t)$, both Equations (12) and (25) are interchangeable because mixing keeps the biomass uniform in the mixed layer (Equation 24). Using expression (Equation 24), we can write the production term in the equation for total biomass as follows:

$$\int_0^{Z_m} Bp^B(I)\mathrm{d}z = \frac{B_Z}{Z_m}\int_0^{Z_m} p^B(I)\mathrm{d}z. \tag{26}$$

We can now expand $B_Z = BZ_m$ in each term in Equation (25) and recover Equation (12). Therefore, the two equations are fundamentally the same, under the assumption that the mixed-layer depth is constant over time.

Central to equations for the time evolution of biomass, be it average (Equation 12), or total biomass (Equation 25), is the production term. As biomass changes, so too does the production term. Under constant surface irradiance, the physical mechanism responsible for a change in the production term is light attenuation caused by biomass. Increasing biomass in the mixed layer reduces the underwater light intensity at all subsurface depths, which then reduces biomass-specific production at each of those depths, and vice versa. This interplay is central to understanding the effect of bio-optical feedback on system stability. To analyze steady-state stability, we first find exact expressions for steady-state biomass, both average B^* and total B_Z^*, where the asterisk * indicates steady state.

Using Equation (5) for irradiance at the mixed layer base $I(Z_m)$ (Figure 3), which for notational simplicity we label as $I_Z = I(Z_m)$, reads as follows:

$$I_Z = I_0 \exp(-(K_w + k_B B) Z_m). \tag{27}$$

Upon taking the time derivative of this expression, we get:

$$\frac{\mathrm{d}I_Z}{\mathrm{d}t} = -\left(k_B Z_m \frac{\mathrm{d}B}{\mathrm{d}t}\right) I_Z. \tag{28}$$

Eliminating time further gives us

$$\frac{\mathrm{d}I_Z}{\mathrm{d}B} = -k_B Z_m I_Z. \tag{29}$$

A general form of this result was first derived by Weissing and Huisman (1994) (their Equation 22). By separation of variables and integration from the initial state (characterized by $B(0)$ and $I_Z(0)$) till the final steady state (characterized by B^* and I_Z^*), we get:

$$B^* = \frac{K_w}{k_B}\left(\frac{1}{K_w Z_m}\ln\frac{I_0}{I_Z^*} - 1\right), \tag{30}$$

as the expression for steady-state biomass. To be dimensionally consistent, the first term in the brackets has to be dimensionless, which implies that the term $\ln\left(I_0/I_Z^*\right)/K_w$ has the dimension of depth. Comparison with the solution for B^* from Kovač et al. (2021) (their Equation 36) shows that the term that carries the dimension of length must in fact be C, the optically uncoupled critical depth. In other words, we have:

$$C = \frac{1}{K_w}\ln\frac{I_0}{I_Z^*}, \tag{31}$$

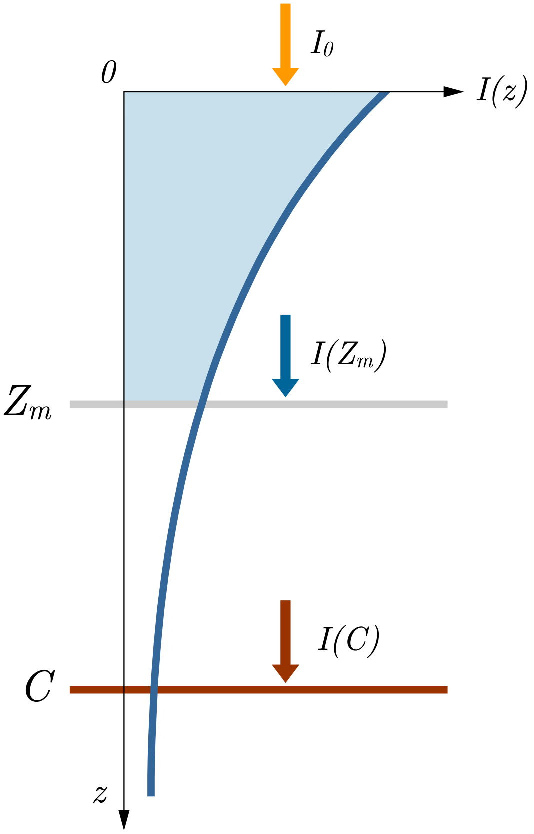

Figure 3. Irradiance at the mixed-layer depth $I(Z_m)$ (blue arrow), calculated from surface irradiance I_0 (orange arrow) attenuated due to water and mixed-layer biomass (Equation 27), at steady equals the irradiance at the optically uncoupled critical depth $I(C)$ (red arrow), even though $Z_m \neq C$.

which is the same as stating $I_Z^* = I_0 \exp(-K_w C)$ or that the steady-state light level corresponds to that at the critical depth for the case of no bio-optical coupling. This expression is consistent with the definition of the critical depth given by Huisman et al. (2002) (their Equation 9). Therefore, by combining the previous two expressions, for the biomass at steady state we get:

$$B^* = \frac{K_w}{k_B}\left(\frac{C}{Z_m} - 1\right), \tag{32}$$

shown in Figure 4. It is important to note that this result is general and does not depend on the specific formulation of the photosynthesis irradiance function. It was first derived by Kovač et al. (2021) for a linear photosynthesis irradiance function. Here, it is generalized to any photosynthesis irradiance function. The production-light relation, as dictated by the photosynthesis irradiance function determines C and therefore B^*. It is important to stress that C is the optically uncoupled critical depth, as defined in Kovač et al. (2021) and not Z_c as defined in Equation (19). More precisely, C is the solution to:

$$\int_0^C p^B(I)\mathrm{d}z = L^B C, \tag{33}$$

under:

$$\frac{\mathrm{d}I}{\mathrm{d}z} = -K_w I, \tag{34}$$

implying bio-optical coupling is not present in the model. Optically coupled critical depth is then the critical depth as defined under bio-optical coupling given in Equation (4), in line with the definitions given in Kovač et al. (2021). With no bio-optical coupling, irradiance at C is simply:

$$I(C) = I_0 \exp(-K_w C). \tag{35}$$

With bio-optical coupling (Equation 4), steady-state irradiance I_Z^* is calculated from Equation (31):

$$I_Z^* = I_0 \exp(-K_w C). \tag{36}$$

From this, we observe that irradiance at the mixed-layer depth at steady state equals the irradiance at the optically uncoupled critical depth:

$$I_Z^* = I(C). \tag{37}$$

This result was already demonstrated for the linear photosynthesis irradiance model by Kovač et al. (2021). Here, it is generalized to any photosynthesis irradiance function. Additionally, due to Equation (23), irradiance at the optically coupled critical depth does not change with time, implying $I(Z_c(t)) = I_Z^*$. Furthermore, because $I_Z^* = I(C)$, we have

$$I(Z_c(t)) = I(C). \tag{38}$$

Therefore, it is $I(C)$, which is in fact a constant of motion.

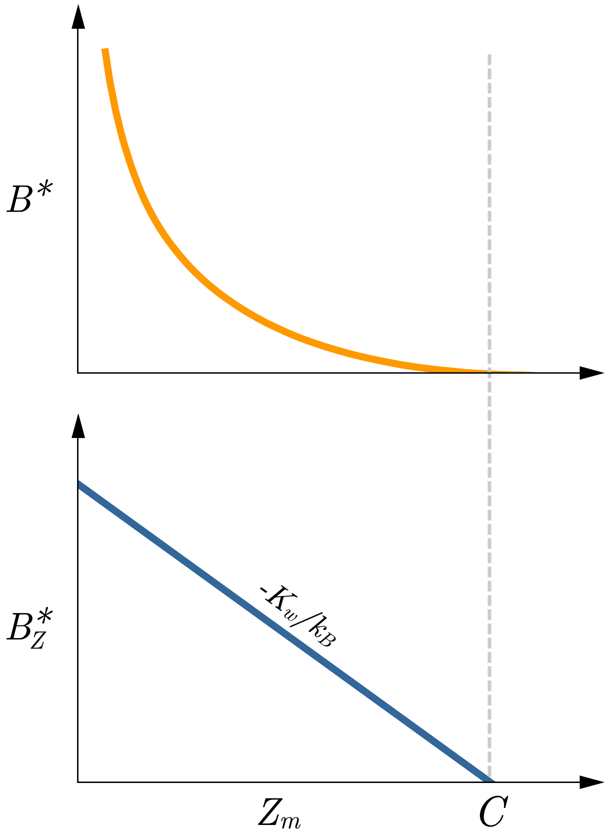

Figure 4. Plot of solutions for average B^* (Equation 32) (orange curve) and total mixed layer biomass B_Z^* (Equation 39) (blue line) at steady state as a function of mixed-layer depth Z_m. When the mixed-layer depth crosses the optically uncoupled critical depth C (dashed line), both average and total biomass go to zero. When the mixed layer goes to zero, average biomass diverges, whereas total biomass goes to $K_w C / k_B$. The slope of the steady-state solution for total biomass (blue line) is given by $-K_w/k_B$.

Finally, having derived the solution for average steady-state biomass, it is straightforward to find the total steady-state biomass, by simply multiplying (Equation 32) with the mixed layer depth:

$$B_Z^* = \frac{K_w}{k_B}(C - Z_m), \tag{39}$$

as shown in Figure 4. According to this equation, total steady-state biomass is proportional to the depth difference between the optically uncoupled critical depth and the mixed-layer depth (Figure 3). Expression (Equation 39) is straightforward to interpret. We can rewrite it as follows:

$$k_B B_Z^* = K_w (C - Z_m). \tag{40}$$

On the left-hand side is the attenuation due to biomass in the mixed layer, and on the right-hand side is the attenuation due to the water column extending from the optically uncoupled critical depth C to Z_m. Because the irradiance at C is constant and $Z_m \neq C$, in order to keep irradiance at the mixed-layer base equal to $I(C)$ at steady state, mixed-layer biomass adjusts so as to match the total attenuation arising only from seawater from Z_m to C. In case of a mixed layer approaching zero the solution gives:

$$\lim_{Z_m \to 0} B_Z^* = \frac{K_w}{k_B} C. \tag{41}$$

This is a finite quantity, in comparison to the solution for average steady-state biomass (Equation 32), which diverges when Z_m goes to zero. Having found the exact expressions for average and total biomass at steady state, we now proceed to analyze their stability.

5. Bio-Optical Bifurcation

Equation (12) describing the time evolution of average biomass can be written as follows:

$$\frac{\mathrm{d}B}{\mathrm{d}t} = f(B), \tag{42}$$

where now the function on the right-hand side equals

$$f(B) = \frac{1}{Z_m} \int_0^{Z_m} B p^B(I) \mathrm{d}z - L^B B. \tag{43}$$

A plot of $f(B)$ is given in Figure 5. At the point where $f(B) = 0$, we have a steady state. In our case, there are two steady states: the trivial steady state $B^* = 0$ and the nontrivial steady state $B^* \neq 0$, given by Equation (32). Either can be stable or unstable. To classify them, we use linear stability analysis. Following Strogatz (2015), in linear stability analysis, the condition for stability reads as follows:

$$\left.\frac{\mathrm{d}f(B)}{\mathrm{d}B}\right|_{B^*} < 0, \tag{44}$$

and the condition for instability reads:

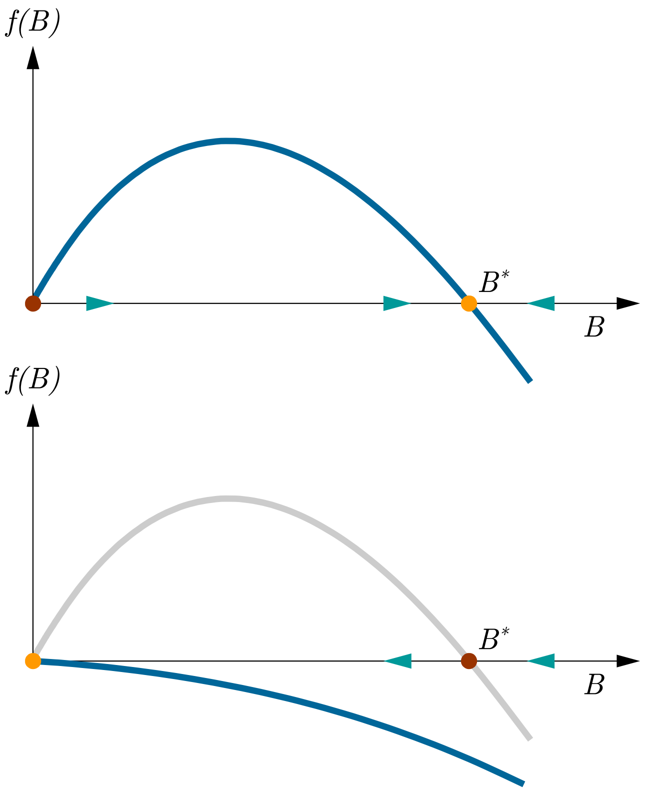

Figure 5. Plot of the $f(B)$ function from Equation (42). Null points of $f(B)$ correspond to steady states: a stable steady state (orange circle) and an unstable steady state (red circle). The situation on top arises when $Z_m < C$ and $B^* > 0$ given by Equation (32) is the stable state, whereas $B^* = 0$ is the unstable state. Once $Z_m > C$, the steady states change stability properties with $B^* = 0$ now becoming stable and $B^* > 0$ now becoming unstable.

$$\left.\frac{\mathrm{d}f(B)}{\mathrm{d}B}\right|_{B^*} > 0. \tag{45}$$

According to these conditions, we observe that the derivative of $f(B)$ determines stability. The derivative of Equation (43) with respect to B is:

$$\frac{\mathrm{d}f(B)}{\mathrm{d}B} = \frac{1}{Z_m}\int_0^{Z_m} p^B(I)\mathrm{d}z + \frac{1}{Z_m}\int_0^{Z_m} B\,\frac{\mathrm{d}p^B(I)}{\mathrm{d}B}\mathrm{d}z - L^B. \tag{46}$$

To evaluate it, one could select a $p^B(I)$ function and carry out the differentiation, which is straightforward to do. An alternative would be to recognize that at steady state, average production equals losses (Equation 15); therefore, the first and the third terms on the right-hand side cancel out at steady state B^*, leaving us with:

$$\left.\frac{\mathrm{d}f(B)}{\mathrm{d}B}\right|_{B^*} = \frac{B^*}{Z_m}\int_0^{Z_m} \left.\frac{\mathrm{d}p^B(I)}{\mathrm{d}B}\right|_{B^*}\mathrm{d}z. \tag{47}$$

Whether or not the steady state is stable depends on the sign of this expression. Looking at Figure 5, we observe that for there to be a nontrivial steady state, the function $f(B)$ has to intersect the B axis at a point B^*, given by Equation (32), implying the derivative of $f(B)$ (Equation 46) has to be negative at the nontrivial steady state and positive at the trivial steady state.

Let us first observe what happens at the trivial steady state, and to this end, let us assume biomass approaches zero. Mathematically, with $B \to 0$, the middle term in Equation (46) vanishes, and we have:

$$\lim_{B\to 0}\frac{\mathrm{d}f(B)}{\mathrm{d}B} = \frac{1}{Z_m}\int_0^{Z_m} p^B(I)\mathrm{d}z - L^B. \tag{48}$$

Physically, the vanishing of that term reflects the fact that at low biomass, the contribution to light attenuation due to biomass is negligible. Now, if the mixed layer is shallower than the critical depth, average mixed-layer production is higher than the loss rate as follows:

$$\frac{1}{Z_m}\int_0^{Z_m} p^B(I)\mathrm{d}z > L^B, \tag{49}$$

and at zero biomass, the slope of $f(B)$ will be positive (Figure 5). This renders the trivial steady state unstable and opens the possibility for the existence of a nontrivial steady state. Using the chain rule in Equation (47) at the nontrivial steady state gives us:

$$\left.\frac{\mathrm{d}f(B)}{\mathrm{d}B}\right|_{B^*} = \frac{B}{Z_m}\int_0^{Z_m} \frac{\mathrm{d}p^B(I)}{\mathrm{d}I}\,\frac{\mathrm{d}I}{\mathrm{d}B}\mathrm{d}z. \tag{50}$$

Following Equation (5), while acknowledging vertically uniform biomass in the mixed layer, we have

$$\frac{\mathrm{d}I}{\mathrm{d}B} = -k_B z I, \tag{51}$$

making the previous expression negative, implying the nontrivial steady state is stable, according to Equation (44). On the contrary, if the opposite of Equation (49) holds, namely:

$$\frac{1}{Z_m}\int_0^{Z_m} p^B(I)\mathrm{d}z < L^B, \tag{52}$$

The slope of $f(B)$ at zero will be negative, and the trivial steady state will be the only stable state (Figure 5).

The nontrivial steady state is stable due to the bio-optical feedback. Without it, the production term would be linear in B, and $f(B)$ would not intersect the B axis. The steady states would either be zero, in case the loss term dominates, or infinity, in case the production term dominates. With the bio-optical feedback, the biomass affects the underwater light field, and for a given mixed-layer depth, higher biomass implies lower irradiance and vice versa. Consequently, lower irradiance implies less production. Therefore, the production term saturates with respect to biomass, while the loss term keeps growing linearly with biomass. Change of biomass per unit time is given as the difference between the two. This implies that the $f(B)$ function has to cross the B axis at some point, which is the nontrivial steady state B^*.

The same reasoning applies to the equation for total biomass, which we can now write as:

$$\frac{\mathrm{d}B_Z}{\mathrm{d}t} = F(B_Z), \tag{53}$$

where the $F(B_Z)$ function equals:

$$F(B_Z) = \frac{B_Z}{Z_m}\int_0^{Z_m} p^B(I)\mathrm{d}z - L^B B_Z. \tag{54}$$

This equation is obtained by multiplying (Equation 42) with the mixed-layer depth Z_m and using Equation (26). From this, we observe that $F(B_Z) = f(B)Z_m$. Therefore, the presented analysis still holds with the difference being in having B_Z^* in place of B^*.

The analysis above provides new insights into the deep connection between the critical depth criterion and the stability of steady states. In this context, the critical depth criterion can be reinterpreted as the criterion for a change in stability properties of the trivial and the nontrivial steady state, as presented in the bifurcation diagram in Figure 6. With the critical depth criterion being met (Equation 49), the nontrivial steady state is stable. With the critical depth criterion not being met (Equation 52), the trivial steady state is stable. In the jargon of dynamical system theory with Z_m crossing C the trivial steady state goes from a source to a sink, whereas the nontrivial steady state goes from a sink to a source (Figure 6). The critical depth C is the bifurcation point for biomass, with the mixed-layer depth Z_m as the bifurcation parameter.

The uncoupled critical depth C is also a bifurcation point for the optically coupled critical depth Z_c (Figure 6). While $Z_m < C$, the optically coupled critical depth converges to the mixed-layer depth at steady state, as demonstrated in Kovač et al. (2021) by solving (Equation 20). Upon Z_m crossing the optically uncoupled critical depth C, biomass goes to zero and attenuation of light is caused only by seawater. This implies that the optically coupled critical depth Z_c has to match the optically uncoupled critical depth C, given that irradiance at the optically coupled critical depth equals the irradiance at the optically uncoupled critical depth $I(Z_c) = I(C)$. The only way in which this can be achieved is if $Z_c = C$ when $Z_m > C$, as shown in Figure 6.

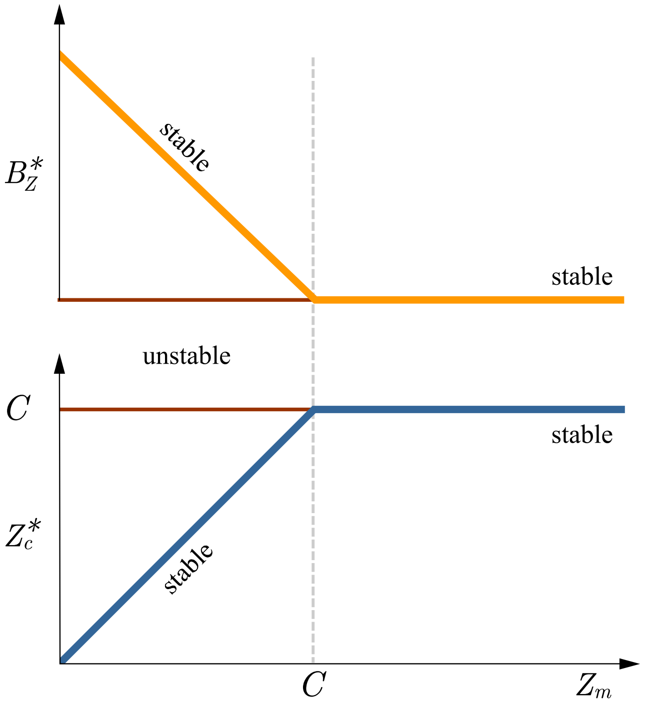

Figure 6. Bifurcation diagram for total biomass B_Z and the optically coupled critical depth Z_c, with the mixed-layer depth Z_m as the bifurcation parameter. For Z_m shallower than the optically uncoupled critical depth C, zero biomass is the unstable steady state (red line) and $B^* > 0$ given by Equation (39) is the stable steady state (orange line). Once Z_m becomes deeper than C, zero biomass becomes the stable steady state (orange line). Mixed-layer depth itself is the stable steady state for Z_c (blue line) when $Z_m < C$, with C as the unstable steady state (red line). When the mixed-layer depth crosses C, it becomes the stable steady state (blue line).

6. Transients

Having found the exact expressions for average and total biomass at steady state and having classified their stability properties, we now explore transients. By transients, we imply time-dependent solutions, which may arise when the system gets perturbed out of a steady state. Such perturbations arise naturally in the ocean due to mixed-layer deepening and shallowing (Mann & Lazier, 2005).

First, assume that mixed-layer biomass is at steady state and also assume zero biomass below the mixed layer, due to unfavorable growth conditions. Let the mixed-layer depth be increasing with time as follows:

$$\frac{\mathrm{d}Z_m}{\mathrm{d}t} > 0. \tag{55}$$

Deepening does not affect total biomass directly (Freilich et al., 2021); therefore Equation (25) still holds, such that:

$$\frac{\partial B_Z}{\partial t} = \int_0^{Z_m(t)} Bp^B(I)\mathrm{d}z - L^B B_Z, \tag{56}$$

now with the recognition that $Z_m = Z_m(t)$. Due to the change in $Z_m(t)$, the production term gets affected and production now changes with time as follows:

$$\frac{\mathrm{d}}{\mathrm{d}t}\int_0^{Z_m(t)} Bp^B(I)\mathrm{d}z = \frac{\mathrm{d}B}{\mathrm{d}t}\int_0^{Z_m(t)} p^B(I)\mathrm{d}z + B\int_0^{Z_m(t)} \frac{\mathrm{d}p^B(I)}{\mathrm{d}t}\mathrm{d}z + Bp^B[I(Z_m(t))]\,\frac{\mathrm{d}Z_m(t)}{\mathrm{d}t}, \tag{57}$$

where biomass comes out of the integral sign due to it being constant with depth in the mixed layer.

The first term on the right-hand side arises simply due to the change in biomass with time. Looking more closely at the integrand in the second term on the right-hand side, we have:

$$\frac{\mathrm{d}p^B(I)}{\mathrm{d}t} = \frac{\mathrm{d}p^B(I)}{\mathrm{d}I}\frac{\mathrm{d}I}{\mathrm{d}t}, \tag{58}$$

where the chain rule was applied. Due to $\mathrm{d}p^B(I)/\mathrm{d}I > 0$, (Platt et al., 1977) the first term in the product is always positive. To arrive at the sign of the second term in the product, we note it is easily calculated by taking the time derivative of Equation (5) to obtain:

$$\frac{\mathrm{d}I}{\mathrm{d}t} = -\left(k_B z\frac{\mathrm{d}B}{\mathrm{d}t}\right)I, \tag{59}$$

which can be both positive or negative, depending on the sign of $\mathrm{d}B/\mathrm{d}t$. Using the derived expressions and taking the $\mathrm{d}B/\mathrm{d}t$ term out of the integral enables us to rewrite the second term in Equation (57) as follows:

$$B\int_0^{Z_m(t)} \frac{\mathrm{d}p^B(I)}{\mathrm{d}t}\mathrm{d}z = -\frac{\mathrm{d}B}{\mathrm{d}t}\int_0^{Z_m(t)} \frac{\mathrm{d}p^B(I)}{\mathrm{d}I}(k_B BI)\,z\,\mathrm{d}z. \tag{60}$$

Now we observe that the second term in Equation (57) arises due to the change in the light field caused by a change in biomass. All the quantities in it are positive, but given the minus sign, the contribution to the change of the production term depends also on the sign of $\mathrm{d}B/\mathrm{d}t$, as expected. Without the bio-optical feedback, which corresponds to $k_B = 0$, this term is zero and there is no feedback of biomass on the light field and subsequently on the production term.

The final term on the right-hand side of Equation (57) arises due to mixed-layer deepening. Mathematically, it is a result of the application of the Leibnitz integral rule. This term does not appear when the mixed-layer depth is constant with time. It reflects the increase in total mixed-layer production resulting from an increase in mixed-layer depth. It is positive, implying it acts to increase total mixed-layer production during deepening.

Whether or not the resulting derivative of total mixed layer production with time will be positive or negative depends on the sum of the three terms in Equation (57). The factor determining this is the sign of $\mathrm{d}B/\mathrm{d}t$. When it is positive, the first term on the right-hand side of Equation (57) is positive and the second one is negative, reflecting the fact that light attenuation is increasing as a result of increasing mixed-layer biomass. However, when it is negative, the first term is negative and the second one is positive, because light attenuation is decreasing as a result of decreasing mixed-layer biomass. Whether or not $\mathrm{d}B/\mathrm{d}t$ will be positive or negative, can be explored by studying the equation for average mixed-layer biomass, which now gets augmented to account for the effect of deepening.

During deepening, average biomass gets diluted due to entrainment of water from below the mixed layer (Behrenfeld & Boss, 2014; Platt, Sathyendranath, et al., 2003). To account for this, an additional term appears in the equation for the time evolution of average biomass (Equation 12):

$$\frac{\partial B}{\partial t} = \frac{1}{Z_m}\int_0^{Z_m} Bp^B(I)\mathrm{d}z - L^B B - \frac{1}{Z_m}\frac{\mathrm{d}Z_m}{\mathrm{d}t}B. \tag{61}$$

Therefore, an asymmetry between Equations (56) and (61) arises. To analyze the consequences of this asymmetry, we explore the response of average and total biomass in the following scenario.

Assume the system is at steady state with mixed-layer depth equal to Z_0 (Figure 7) and the corresponding average biomass given by Equation (32) with total biomass given by Equation (39). Deepening of Z_m will then change the steady state, and following Equations (32) and (39) in both cases, the new steady state biomass is B_d, where the subscript stands for deep, and will be lower in biomass, both average and total biomass, given that the final mixed-layer depth is deeper than the initial $Z_d > Z_0$ (see also Figure 6). If the final mixed-layer depth is shallower than C, the new steady state is stable (Figure 6). Therefore, biomass is attracted toward the new steady state with average and total biomass both declining during the transition to a deeper mixed layer. However, if the system is not initially at steady state, biomass may either decline or increase with time, depending on the initial condition in relation to the final steady-state biomass. When $B_0 < B_d$, biomass may be increasing even during deepening, a process, which classically is expected to occur only during shallowing.

To explore the dynamical response to shallowing, assume that mixed-layer depth decreases with time as follows:

$$\frac{\mathrm{d}Z_m}{\mathrm{d}t} < 0. \tag{62}$$

Shallowing does not affect average biomass directly; therefore, Equation (12) still holds:

$$\frac{\partial B}{\partial t} = \frac{1}{Z_m(t)}\int_0^{Z_m(t)} Bp^B(I)\mathrm{d}z - L^B B, \tag{63}$$

again with the recognition that $Z_m = Z_m(t)$. Although average biomass is not affected directly by shallowing, the production term is, and therefore, subsequently, biomass is affected. To see how the production term changes in

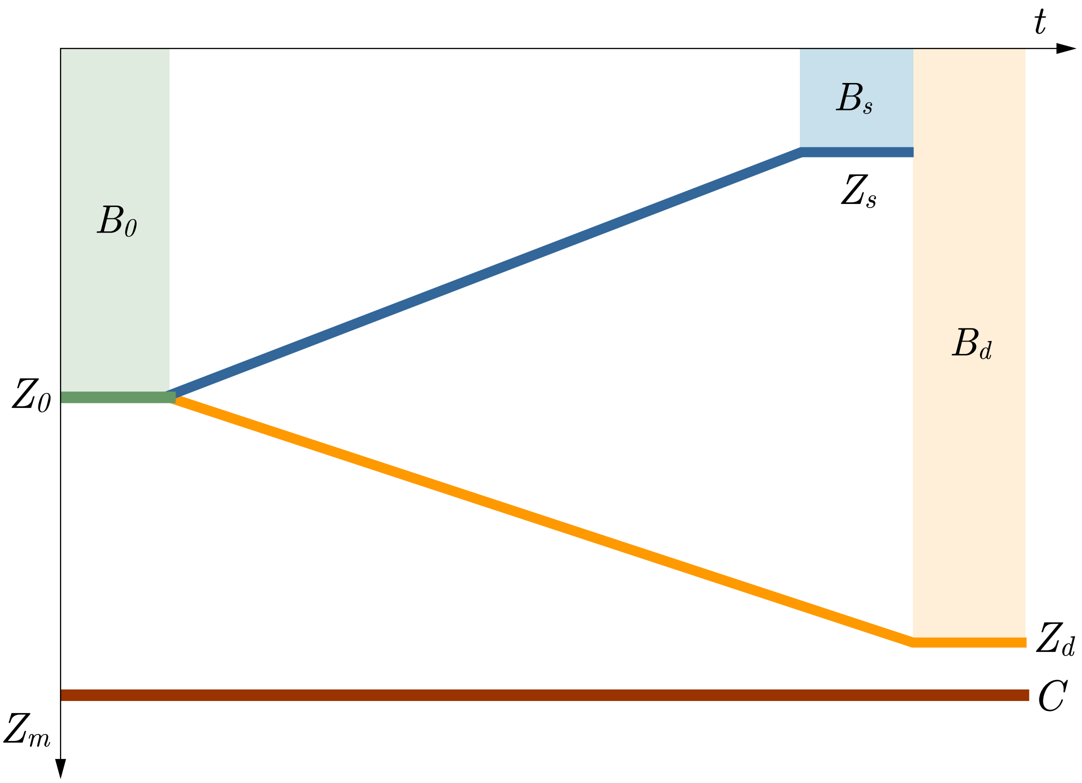

Figure 7. Response of mixed-layer biomass to changing mixed-layer depth under $Z_m(t) < C$. The system is initially at steady state with average biomass B_0, given by Equation (32). During mixed-layer deepening (orange line), biomass changes with time. After deepening stops, the system acquires a new steady state with average biomass B_d, which following Equation (32) is less than B_0. Following Equation (39), the same argument holds for total biomass. Response of mixed-layer biomass to shallowing is also shown (blue line). After shallowing stops, the system acquires a new steady state with average biomass B_s, which following Equation (32) is higher than B_0. Following Equation (39), the same argument holds for total biomass.

response to shallowing, we can explore this change in the same manner as was done with expression (Equation 57) as follows:

$$\frac{\mathrm{d}}{\mathrm{d}t}\int_0^{Z_m} Bp^B(I)\mathrm{d}z = \frac{\mathrm{d}B}{\mathrm{d}t}\int_0^{Z_m(t)} p^B(I)\mathrm{d}z + B\int_0^{Z_m(t)} \frac{\mathrm{d}p^B(I)}{\mathrm{d}t}\mathrm{d}z - Bp^B[I(Z_m(t))]\left|\frac{\mathrm{d}Z_m(t)}{\mathrm{d}t}\right|, \tag{64}$$

with the difference that now the time derivative of the mixed-layer depth has a negative sign and to emphasize it we use the absolute value of the change in mixed-layer depth per unit time. The third term on the right-hand side now reflects the decrease in total mixed-layer production resulting from a decrease in mixed-layer depth. It is negative, implying it acts to decrease total mixed-layer production during shallowing. This occurs due to detrainment of biomass from the mixed layer during shallowing. The biomass which now finds itself below the mixed layer no longer contributes to mixed-layer production (Edwards et al., 2004).

In this line of reasoning, total biomass is affected by shallowing directly, because a portion of biomass gets detrained from the mixed layer and the equation for total biomass (Equation 25) now becomes (Freilich et al., 2021)

$$\frac{\partial B_Z}{\partial t} = \int_0^{Z_m(t)} Bp^B(I)\mathrm{d}z - L^B B_Z - \frac{1}{Z_m}\left|\frac{\mathrm{d}Z_m}{\mathrm{d}t}\right| B_Z. \tag{65}$$

Therefore, once again, an asymmetry arises between Equations (63) and (65). Whereas during deepening it was the equation for average biomass in which an additional term appeared, now it is in the equation for total biomass that an additional term appears. Here too, in order to analyze the consequences of the asymmetry in the equations for average and total biomass, we explore the response of biomass in the following scenario.

Assume again that the system is at steady state when mixed-layer depth equals Z_0 (Figure 7), that the corresponding average biomass is given by Equation (32), and total biomass given by Equation (39). Shallowing of the mixed layer will then change the steady state B_s, both average and total biomass, where the subscript stands for shallow, because $Z_s < Z_0$ (see also Figure 6). Because the new steady state is stable, the system will tend toward this new steady state and average and total biomass will both increase with time. However, if the system is not initially at steady state, biomass may either decline or increase with time depending on the initial condition in relation to the final steady state. When $B_0 > B_s$, biomass may be decreasing even during shallowing.

The response of the system to both deepening and shallowing can be interpreted using the notion of the optically coupled critical depth. The optically coupled critical depth will converge toward the mixed-layer depth in both cases. If initially at steady state, the optically coupled critical depth equals the mixed-layer depth $Z_c = Z_0$. During shallowing, Z_c will change and once the mixed layer settles onto the new depth Z_s, the optically coupled critical depth will continue changing with time until it too equals this new mixed layer depth $Z_c = Z_s$.

The response to deepening proceeds along the same lines with the optically coupled critical depth now converging toward Z_d. If initially at steady state the optically coupled critical depth will be equal to the mixed-layer depth $Z_c = Z_0$. During deepening, Z_c will change, and once the mixed layer settles onto the new depth, Z_c will continue changing with time until it too equals this new mixed-layer depth. At this point, the system has reached steady state with $Z_c = Z_m$ and biomass being equal to B_d.

7. Discussion

Phytoplankton are at the mercy of their physical environment, surviving in the euphotic zone, the well-lit uppermost part of the ocean where sufficient light is available for photosynthesis (Kirk, 2011; Mann & Lazier, 2005). Gravity causes phytoplankton to sink, therefore effectively acting to remove nonbuoyant phytoplankton from the euphotic zone (Huisman & Sommeijer, 2002b). Complementary to sinking is the process of turbulent mixing, which may act twofold. In case of weak mixing, it may suppress the sinking tendencies of phytoplankton, thereby aiding phytoplankton cells to stay in the euphotic zone (Huisman & Sommeijer, 2002a), which is favorable for primary production. However, in case of strong mixing, say caused by deep convection, phytoplankton cells may get dragged to a great depth, where they experience low light intensities, subsequently reducing primary production in the mixed layer (Franks, 2015). In the ocean, mixing depth and mixing intensity naturally vary depending on the source of turbulence (Franks, 2015).

In his original paper, Sverdrup (1953) assumed instantaneous mixing, with the mixed-layer depth as the only parameter associated with mixing. Therefore, the only question such a model could answer is how deep active mixing could be, while still keeping production above the loss rate, because there was no parameter to vary the intensity of mixing. This meant that when the mixed layer was shallow, such that light levels in the mixed layer were sufficient for production to surpass the loss rate, the conditions were met for bloom initiation, given that no other mechanism existed in the model to trigger a bloom. It also meant the converse. With deep mixing, average light levels were low in the mixed layer and the loss rate surpassed production, preventing bloom initiation. The mixed-layer depth at which the production in the layer matched corresponding losses was defined by Sverdrup (1953) as the critical depth.

Almost half a century later, Huisman et al. (1999a) extended Sverdrup's theory by taking into account varying mixing intensities and demonstrated that under weak mixing production can exceed the combined effects of mixing and losses, enabling phytoplankton to be sustained in the water column even in case of no stratification. They also included the effect of sinking (Huisman et al., 2002). In the case of strong mixing, predictions given by Huisman et al. (1999a) agreed with those of Sverdrup (1953). In this way, the model of Sverdrup (1953) can be viewed as the particular case of the Huisman et al.'s (1999a) model for strong mixing.

The now standard mathematical framework used by Huisman et al. (1999a), which dates back to the work of Riley et al. (1949), is to model the processes of sinking, mixing, production and losses, with an advection-diffusion-reaction equation for the phytoplankton biomass as a function of depth (Ryabov & Blasius, 2008). The advection and diffusion terms account for sinking and mixing, whereas the reaction terms account for biological processes and come with a number of parametrizations (Franks, 2002). The key parametrization from the standpoint of optics is the photosynthesis irradiance function (Kovač et al., 2017). Mathematically, it relates light availability at depth to primary production at depth and enables the growth of phytoplankton in the model.

To calculate production, a light penetration model is needed. In the light model, surface light, and optical properties of seawater and other optically important substances in the water, including phytoplankton, at all depths above a given depth determine the light intensity at that depth, making the system nonlocal. A light model in which biomass affects the underwater light field adds an integral equation to the advection-diffusion-reaction equation for biomass. The two equations are coupled via the effect of phytoplankton on the attenuation coefficient, so that changes in biomass affect the underwater light field and subsequently production, which then feeds back onto biomass. Without this coupling, biomass would not affect the underwater light field, and it is precisely the dynamical consequences caused by the effect of biomass on the underwater light field that are often ignored in many models, but are the main focus of this study.

Dynamically, the bio-optical feedback creates a nontrivial (biomass greater than zero) steady state for the mixed-layer biomass (Figure 5), which otherwise would not exist and is therefore in itself an important distinction from a model not having a steady state. The existence of such a steady state was first recognized by Platt, Sathyendranath, et al. (2003), and its dynamic consequences were studied further in Platt, Sathyendranath, et al. (2003), Edwards et al. (2004), and Kovač et al. (2020, 2021). In the work of Kovač et al. (2021), an exact expression for the nontrivial steady state was derived for a model with a linear photosynthesis irradiance function, but which is in other respects same as the model in this paper.

Here, it was demonstrated that the steady-state solution is not dependent on the specific form of the photosynthesis irradiance function and is general for all functions, linear and nonlinear. Mathematically, the exact form of the photosynthesis irradiance function determines the value of C in the expression for steady-state biomass (Equation 32), but does not alter its form. In that sense, it is valid for the whole class of photosynthesis irradiance functions. The steady-state solution for total mixed-layer biomass was also derived here (Equation 39), which was thus far unknown. By doing so, the issue of average biomass diverging for mixed-layer depth going to zero was remedied, given that the steady-state solution for total biomass (Equation 39) does not exhibit the same divergent behavior.

The Critical Depth Conservation Principle, whereby the product of the attenuation coefficient and the critical depth is a constant of motion, was also discovered for a linear photosynthesis irradiance function by Kovač et al. (2021). Here, it was demonstrated to hold irrespective of the photosynthesis irradiance function used in the model. This was demonstrated simply by observing changes in light intensity through the water column in a novel fashion. The standard way to do this is to observe how light intensity changes at a given depth. However, because irradiance declines with depth, the $I(z)$ function is a bijection, such that for each irradiance value, a corresponding depth value can be assigned and how that assigned depth changes over time can be observed. This reasoning also led to the derivation of a general equation for the time evolution of the compensation depth (Equation 10), thus far unknown. The equation demonstrates that the integral biomass above the compensation depth changes with time while keeping the irradiance at the compensation depth constant. In this case, the integral of the attenuation coefficient from the surface up to the compensation depth is a constant of motion (Equation 9). The derived constants of motion are another direct consequence of the bio-optical feedback, which arises due to the attenuation of light caused by phytoplankton.

In the model of Sverdrup (1953), the bio-optical feedback was not accounted for and the underwater light field was not affected by phytoplankton. Therefore, the argument of growth/decline of biomass was framed solely in terms of the relation between the critical depth and the mixed-layer depth. The same argument was also framed by Huisman and Weissing (1994) and Weissing and Huisman (1994) in terms of the critical light intensity. However, in their model, the underwater light field was affected by biomass. Recently, the two approaches were merged in the work of Kovač et al. (2021) where it was shown that the critical light intensity equals the light intensity at the critical depth at steady state. In the model of Kovač et al. (2021), the underwater light field is affected by both seawater (and any other, fixed, background attenuation by substances that do not covary with phytoplankton) and biomass.

It is worth stressing that the effect biomass has on the underwater light field also modulates bloom dynamics in the following manner. The bloom may be triggered or terminated by both bottom-up or top-down controls. The bottom-up would be nutrient limitation, whereas the top-down would be zooplankton grazing (Lynam et al., 2016). To model either top-down or bottom-up controls, the system has to be extended to at least two dimensions, with the second arising from the equation for nutrients or zooplankton. When both limitations are taken into account, the system is extended to three dimensions, the classical example of which are the nutrient-phytoplankton-zooplankton models (Fasham et al., 1990; Franks, 2002; Franks et al., 1986). The interplay between nutrients, phytoplankton, and zooplankton regulates the bloom mechanism and causes bloom onset or termination. It would be difficult to classify light limitation as either bottom-up or top-down control, and could be labelled self-limitation. In this respect, the bio-optical feedback is a self-regulating mechanism for bloom initiation and termination, with the optically uncoupled critical depth being a bifurcation point for the mixed-layer depth (Figure 6). In the jargon of dynamical systems theory, bio-optical feedback causes the existence of a stable sink fixed point when the critical depth criterion is met. Mixed layer crossing the optically uncoupled critical depth amounts to the annihilation of the stable sink fixed point, with the trivial steady state being the only attractive attracting fixed point left. For mixed layers that extend beyond the optically uncoupled critical depth, biomass eventually goes to zero, because there is no steady state with positive biomass. This occurs because the average light level in the mixed layer, with no biomass present, is only controlled by the mixed-layer depth, and drops below the light level needed for production to match the loss rate.

Apart from having the control of the average light level in the mixed layer, the process of mixed-layer deepening also has an effect on the loss rate, as pointed out by Behrenfeld (2010). Due to biomass dilution upon deepening, the phytoplankton-zooplankton encounter rates are diminished, causing a reduction in grazing pressure, which may lead to a bloom onset even during deepening (Behrenfeld & Boss, 2014, 2017). With the bio-optical feedback in place, dilution also reduces the attenuation coefficient. This may then lead to an increase in the average light level in the mixed layer and whether or not this will consequently lead to an increase in average production and subsequently biomass depends not only on how deep the mixed layer is but also on the biomass prior to deepening.

Now, if the biomass prior to deepening is larger than the steady-state biomass associated with the deeper state then biomass will decline as a result of deepening (Figure 7). However, if the biomass prior to deepening is lower than the steady-state biomass associated with the deeper state, then biomass will increase (Figure 7). Therefore, due to the bio-optical feedback, biomass may increase even during deepening. Such a process cannot occur without the bio-optical feedback in a model having only biomass as the single-state variable. For it to take place in a model that does not have the bio-optical feedback in place, it is necessary to include either an equation for nutrients or zooplankton, or both. Modelling nutrients allows for entrainment of nutrient-rich deep water to the mixed layer, elevating nutrient concentrations, which acts to increase production (Platt, Sathyendranath, et al., 2003). Adding zooplankton enables the dilution recoupling mechanism, which acts to decrease grazing upon deepening. In both cases, more than one state variable, apart from biomass, is needed in the model to achieve growth upon deepening.

The described model behavior also emphasizes the need for awareness and caution at model selection, especially when it comes to model data comparisons. Many dynamical models nowadays are compared against remote sensing data. When it comes to chlorophyll, as an index of phytoplankton biomass, such remote sensing data are acquired in the visible part of the spectrum, because it is the photons from this part of the spectrum, which are affected by chlorophyll and used in photosynthesis. To use such data in model data comparisons, it would be reasonable that the light penetration submodels have at least the elementary treatment of the effect phytoplankton have on the underwater light filed. Drawing conclusions from remote sensing data, which are based on light absorption and scattering, about a model which does not have in it the effect of phytoplankton absorption and scattering on the light field may simply be lacking, given that the effect of phytoplankton on the light field is what enables remote sensing of phytoplankton in the first place.

8. Conclusions

In 1953, Sverdrup introduced the concept of a critical depth and thereby provided invaluable early insights into the mechanism of phytoplankton blooms. Critical depth is a depth horizon for the mixed layer and if mixing extends beyond it, light levels in the mixed layer become insufficient for photosynthesis to outpace losses. For mixing not extending to the critical depth, the reverse holds. A related notion, the compensation depth, is relevant when mixing is weak, as it represents the point at which photosynthesis matches the loss rate at depth. To this day, the ideas put together in the original paper of Sverdrup (1953) permeate the literature, as evident by the high number of citations of the original work (Sathyendranath et al., 2015).

The paper presented here has extended the mathematical apparatus underlying the original work of Sverdrup (1953) by examining the impact of self-shading, which introduces a bio-optical feedback into the mathematical model. As a result of this analysis, a new differential equation was derived to describe the time evolution of the compensation depth. By employing the new equation, it was demonstrated that light intensities at both the compensation depth and the critical depth remain constant over time due to the bio-optical feedback within the mixed layer.

The paper has also provided exact solutions for the average and total mixed-layer biomass at steady state and has analyzed their stability properties. A bio-optical bifurcation has been discovered, with the mixed-layer depth acting as the bifurcation parameter. The critical depth has been pinpointed as the bifurcation point where the stability properties of the trivial and nontrivial steady states change. It was shown that the nontrivial steady state is stable when the critical depth criterion is met, whereas the trivial steady state is stable when the critical depth criterion is not met. The paper also explored transients between steady states and emphasized the crucial role of the initial condition in determining whether changes in mixed-layer depth result in an increase or a decrease in biomass over time.

The presented analysis bears relevance in the study of climate tipping points, which are often defined with respect to a threshold temperature (Armstrong McKay et al., 2022). With respect to phytoplankton, we see here that the system stability depends on light available for photosynthesis and on the bio-optical coupling between primary production and mixed-layer dynamics, which in turn depends on surface winds. An earlier paper (Kovač et al., 2020) had also demonstrated the role of nutrient limitation on stability of phytoplankton. It would be difficult to link changes in light, winds, or nutrients directly or indirectly to temperature, without a large number of intermediate steps at best; and as demonstrated here, a more direct route to assessing stability in phytoplankton would be to investigate the coupling between light and phytoplankton in relation to mixed-layer depth. The results suggest that bifurcation in phytoplankton depends on the relationship between mixed-layer depth and critical depth. In the climate change context, the condition of mixed-layer becoming greater than the uncoupled critical depth would trigger a decrease in biomass, with zero biomass becoming an attracting fixed point: persistence of such extreme conditions would be an early signal that the system is under threat during that period. Note that the bifurcation analyzed here is not an irreversible process: a decrease in mixed-layer depth could reverse it. Employing state-of-the-art-coupled hydrodynamic-biogeochemical models to investigate such scenarios is a potential course for future research. In this context also, the concept of critical depth provides a framework to investigate such pressing questions of the day.

Data Availability Statement

This is a theoretical paper, and no experimental data have been used in it.

Acknowledgments
This work was supported by the Croatian Science Foundation under the project number IP-2022-10-8859. This work was supported by the Simons Collaboration on Computational Biogeochemical Modeling of Marine Ecosystems/CBIOMES (549947 to S.S.) on. This work is also a contribution to the Tipping points and abrupt changes In the Marine Ecosystem (TIME) project of the European Space Agency (4000147354/25/I-LR).

References

Armstrong McKay, D. I., Staal, A., Abrams, J. F., Winkelmann, R., Sakschewski, B., Loriani, S., et al. (2022). Exceeding 1.5°c global warming could trigger multiple climate tipping points. *Science*, *377*(6611), 1171. https://doi.org/10.1126/science.abn7950

Behrenfeld, M. J. (2010). Abandoning sverdrup's critical depth hypothesis on phytoplankton blooms. *Ecology*, *91*(4), 977–989. https://doi.org/10.1890/09-1207.1

Behrenfeld, M. J., & Boss, E. S. (2014). Resurrecting the ecological underpinnings of ocean plankton blooms. *Annual Review of Marine Science*, *6*(1), 167–194. https://doi.org/10.1146/annurev-marine-052913-021325

Behrenfeld, M. J., & Boss, E. S. (2017). Student's tutorial on bloom hypotheses in the context of phytoplankton annual cycles. *Global Change Biology*, *24*(1), 55–77. https://doi.org/10.1111/gcb.13858

Behrenfeld, M. J., Doney, S. C., Lima, I., Boss, E. S., & Siegel, D. A. (2013a). Annual cycles of ecological disturbance and recovery underlying the subarctic atlantic spring plankton bloom. *Global Biogeochemical Cycles*, *27*(2), 526–540. https://doi.org/10.1002/gbc.20050

Behrenfeld, M. J., Doney, S. C., Lima, I., Boss, E. S., & Siegel, D. A. (2013b). Reply to a comment by Stephen M. Chiswell on: "Annual cycles of ecological disturbance and recovery underlying the subarctic Atlantic spring plankton bloom" by M. J. Behrenfeld et al. (2013). *Global Biogeochemical Cycles*, *27*, 1294–1296. https://doi.org/10.1002/2013GB004720

Chiswell, S. M. (2011). Annual cycles and spring blooms in phytoplankton: Don't abandon sverdrup completely. *Marine Ecology Progress Series*, *443*, 39–50. https://doi.org/10.3354/meps09453

Chiswell, S. M. (2013). Comment on "annual cycles of ecological disturbance and recovery underlying the subarctic atlantic spring plankton bloom". *Global Biogeochemical Cycles*, *27*(4), 1291–1293. https://doi.org/10.1002/2013GB004681

Chiswell, S. M., Calil, P. H. R., & Boyd, P. W. (2015). Spring blooms and annual cycles of phytoplankton: A unified perspective. *Journal of Plankton Research*, *37*(3), 500–508. https://doi.org/10.1093/plankt/fbv021

Cropp, R., Moroz, I. M., & Norbury, J. (2014). Chaotic dynamics in a simple dynamical green ocean plankton model. *Journal of Marine Systems*, *139*, 483–495. https://doi.org/10.1016/j.jmarsys.2014.08.002

Duarte, C. M., Regaudie-de Gioux, A., Arrieta, J. M., Delgado-Huertas, A., & Agusti, S. (2013). The oligotrophic ocean is heterotrophic. *Annual Review of Marine Science*, *5*(1), 551–569. https://doi.org/10.1146/annurev-marine-121211-172337

Edwards, A. E., Platt, T., & Sathyendranath, S. (2004). The high-nutrient, low-chlorophyll regime of the ocean: Limits on biomass and nitrate before and after iron enrichment. *Ecological Modelling*, *171*(1–2), 103–125. https://doi.org/10.1016/j.ecolmodel.2003.06.001

Fasham, M. J. R., Ducklow, H. W., & McKelvie, S. M. (1990). A nitrogen-based model of plankton dynamics in the oceanic mixed layer. *Journal of Marine Research*, *48*(3), 591–639. https://doi.org/10.1357/002224090784984678

Field, C. B., Behrenfeld, M. J., Randerson, J. T., & Falkowski, P. (1998). Primary production of the biosphere: Integrating terrestrial and oceanic components. *Science*, *281*(5374), 237–240. https://doi.org/10.1126/science.281.5374.237

Franks, P. J. S. (2002). NPZ models of plankton dynamics: Their construction, coupling to physics, and application. *Journal of Oceanography*, *58*(2), 379–387. https://doi.org/10.1023/a:1015874028196

Franks, P. J. S. (2015). Has sverdrup's critical depth hypothesis been tested? Mixed layers vs. turbulent layers. *ICES Journal of Marine Science*, *72*(6), 1897–1907. https://doi.org/10.1093/icesjms/fsu175

Franks, P. J. S., Wroblewski, J. S., & Frierl, G. R. (1986). Behavior of a simple plankton model with food-level acclimation by herbivores. *Marine Biology*, *91*(1), 121–129. https://doi.org/10.1007/BF00397577

Freilich, M., Mignot, A., Flierl, G., & Ferrari, R. (2021). Grazing behavior and winter phytoplankton accumulation. *Biogeosciences*, *18*(20), 5595–5607. https://doi.org/10.5194/bg-18-5595-2021

Gran, H. H., & Braarud, T. (1935). A quantitative study on the phytoplankton of the bay of fundy and the gulf of Maine (including observations on hydrography, chemistry and morbidity). *Journal of the Biological Board of Canada*, *1*, 219–467.

Huisman, J., Arrayas, M., Ebert, U., & Sommeijer, B. (2002). How do sinking phytoplankton species manage to persist? *The American Naturalist*, *159*(3), 245–254. https://doi.org/10.1086/338511

Huisman, J., Pham Thi, N. N., Karl, D. M., & Sommeijer, B. (2006). Reduced mixing generates oscillations and chaos in the oceanic deep chlorophyll maximum. *Nature*, *439*(7074), 322–325. https://doi.org/10.1038/nature04245

Huisman, J., & Sommeijer, B. (2002a). Maximal sustainable sinking velocity of phytoplankton. *Marine Ecology Progress Series*, *244*, 39–48. https://doi.org/10.3354/meps244039

Huisman, J., & Sommeijer, B. (2002b). Population dynamics of sinking phytoplankton in light-limited environments: Simulation techniques and critical parameters. *Journal of Sea Research*, *48*(2), 83–96. https://doi.org/10.1016/S1385-1101(02)00137-5

Huisman, J., van Oostveen, P., & Weissing, F. J. (1999a). Critical depth and critical turbulence: Two different mechanisms for the development of phytoplankton blooms. *Limnology & Oceanography*, *44*(7), 1781–1787. https://doi.org/10.4319/lo.1999.44.7.1781

Huisman, J., van Oostveen, P., & Weissing, F. J. (1999b). Species dynamics in phytoplankton blooms: Incomplete mixing and competition for light. *The American Naturalist*, *154*(1), 46–68. https://doi.org/10.1086/303220

Huisman, J., & Weissing, F. (2001). Fundamental unpredictability in multispecies competition. *The American Naturalist*, *157*(5), 489–494. https://doi.org/10.1086/319929

Huisman, J., & Weissing, F. J. (1994). Light-limited growth and competition for light in well-mixed aquatic environments: An elementary model. *Ecology*, *75*(2), 507–520. https://doi.org/10.2307/1939554

Jassby, A. D., & Platt, T. (1976). Mathematical formulation of the relationship between photosynthesis and light for phytoplankton. *Limnology & Oceanography*, *21*(4), 540–547. https://doi.org/10.4319/lo.1976.21.4.0540

Kirk, J. T. O. (2011). *Light and photosynthesis in quatic ecosystems*. (3rd ed.). Cambridge University Press. https://doi.org/10.1017/CBO9780511623370

Kovač, Z., Platt, T., & Sathyendranath, S. (2020). Stability and resilience in a nutrient-phytoplankton marine ecosystem model. *ICES Journal of Marine Science*, *77*(4), 1556–1572. https://doi.org/10.1093/icesjms/fsaa067

Kovač, Z., Platt, T., & Sathyendranath, S. (2021). Sverdrup meets lambert: Analytical solution for sverdrup's critical depth. *ICES Journal of Marine Science*, fsab013. https://doi.org/10.1093/icesjms/fsaa067

Kovač, Z., Platt, T., Sathyendranath, S., Morović, M., & Jackson, T. (2016). Recovery of photosynthesis parameters from *in situ* profiles of phytoplankton production. *ICES Journal of Marine Science*, *73*(2), 275–285. https://doi.org/10.1093/icesjms/fsv204

Kovač, Z., Platt, T. S. S., Antunović, S., & Antunović, S. (2017). Models for estimating photosynthesis parameters from in situ production profiles. *Progress in Oceanography*, *159*, 255–266. https://doi.org/10.1016/j.pocean.2017.10.013

Kovač, Z., Platt, T. S. S., Morović, M., & Morović, M. (2016). Analytical solution for the vertical profile of daily production in the ocean. *Journal of Geophysical Research: Oceans*, *121*(5), 3532–3548. https://doi.org/10.1002/2015JC011293

Kulk, G., Platt, T., Dingle, J., Jackson, T., Johnsson, B., Bouman, H. A., et al. (2020). Primary production, an index of climate change in the ocean: Satellite-based estimates over two decades. *Remote Sensing*, *12*(5), 826. https://doi.org/10.3390/rs12050826

Kulk, G., Platt, T., Dingle, J., Jackson, T., Johnsson, B., Bouman, H. A., & Sathyendranath, S. (2021). Correction: Primary production, an index of climate change in the ocean: Satellite-based estimates over two decades. *Remote Sensing*, *13*(17), 3462. https://doi.org/10.3390/rs13173462

Laufkötter, C., Vogt, M., & Gruber, N. (2013). Long-term trends in ocean plankton production and particle export between 1960–2006. *Biogeosciences*, *10*(11), 7373–7393. https://doi.org/10.5194/bg-10-7373-2013

Laufkötter, C., Vogt, M., Gruber, N., Aita-Noguchi, M., Aumont, O., Bopp, L., et al. (2015). Drivers and uncertainties of future global marine primary production in marine ecosystem models. *Biogeosciences*, *12*(23), 6955–6984. https://doi.org/10.5194/bg-12-6955-2015

Lenton, T. M., Benson, S., Smith, T., Ewer, T., Lanel, V., Petykowski, E., et al. (2022). Operationalising positive tipping points towards global sustainability. *Global Sustainability*, *5*(e1), 1–16. https://doi.org/10.1017/sus.2021.30

Longhurst, A., Sathyendranath, S., Platt, T., & Caverhill, C. (1995). An estimate of global primary production in the ocean from satellite radiometer data. *Journal of Plankton Research*, *17*(6), 1245–1271. https://doi.org/10.1093/plankt/17.6.1245

Lynam, C. P., Llope, M., Mollmann, C., Helaoutet, P., Bayliss-Brown, G. A., & Stenseth, N. C. (2016). Interaction between top-down and bottom-up control in marine food webs. *Proceedings of the National Academy of Sciences*, *114*(8), 1952–1957. https://doi.org/10.1073/pnas.1621037114

Mann, K. H., & Lazier, J. R. N. (2005). *Dynamics of marine ecosystems*. (3rd ed.). Blackwell Publishing. https://doi.org/10.1002/9781118687901

Ott, E. (2002). *Chaos in dynamical systems*. (2nd ed.). Cambridge University Press. https://doi.org/10.1017/CBO9780511803260

Platt, T., Bird, D. F., & Sathyendranath, S. (1991). Critical depth and marine primary production. *Proceeding of the Royal Society B*, *246*, 205–217.

Platt, T., Broomhead, D. S., Sathyendranath, S., Edwards, A. M., & Murphy, E. J. (2003). Phytoplankton biomass and residual nitrate in the pelagic ecosystem. *Proceeding of the Royal Society A*, *459*(2033), 1063–1073. https://doi.org/10.1098/rspa.2002.1079

Platt, T., Denman, K. L., & Jassby, A. D. (1977). Modelling the productivity of phytoplankton. In *The sea: Ideas and observations on progress in the study of the seas* (pp. 807–856). Wiley.

Platt, T., Lewis, M., & Geider, R. (1984). Thermodynamics of the pelagic ecosystem: Elementary closure conditions for biological production in the open ocean. In *Flows of energy and materials in marine ecosystems* (pp. 49–84). Springer. https://doi.org/10.1007/978-1-4757-0387-0_3

Platt, T., & Sathyendranath, S. (1988). Oceanic primary production: Estimation by remote sensing at local and regional scales. *Science*, *241*(4873), 1613–1620. https://doi.org/10.1126/science.241.4873.1613

Platt, T., & Sathyendranath, S. (1991). Biological production models as elements of coupled, atmosphere-ocean models for climate research. *Journal of Geophysical Research*, *96*(C2), 2585–2592. https://doi.org/10.1029/90JC02305

Platt, T., Sathyendranath, S., Edwards, A. M., Broomhead, D. S., & Ulloa, O. (2003). Nitrate supply and demand in the mixed layer of the ocean. *Marine Ecology Progress Series*, *254*, 3–9. https://doi.org/10.3354/meps254003

Raven, J. A., & Falkowski, P. G. (1999). Oceanic sinks for atmospheric co2. *Plant, Cell and Environment*, *22*(6), 741–755. https://doi.org/10.1046/j.1365-3040.1999.00419.x

Regaudie-de Gioux, A., Lasternas, S., Agusti, S., & Duarte, C. M. (2014). Comparing marine primary production estimates through different methods and development of conversion equations. *Frontiers in Marine Science*, *1*(19), 1–14. https://doi.org/10.3389/fmars.2014.00019

Riley, G. A., Stommel, H., & Bumpus, D. F. (1949). Quantitative ecology of the plankton of the western north atlantic. *Bulletin of the Bingham Oceanographic Collection*, *3*, 1–169.

Rocha, J. C. (2022). Ecosystems are showing symptoms of resilience loss. *Environmental Research Letters*, *17*(6), 065013. https://doi.org/10.1088/1748-9326/ac73a8

Ryabov, A. B., & Blasius, B. (2008). Population growth and persistence in a heterogeneous environment: The role of diffusion and advection. *Mathematical Modelling of Natural Phenomena*, *3*, 42–86. https://doi.org/10.1051/mmnp:2008064

Sathyendranath, S., Ji, R., & Browman, H. I. (2015). Revisiting Sverdrup's critical depth hypothesis. *ICES Journal of Marine Science*, *72*(6), 1892–1896. https://doi.org/10.1093/icesjms/fsv110

Sathyendranath, S., Platt, T., Kovač, Z., Dingle, J., Jackson, T., Brewin, R. J. W., et al. (2020). Reconciling models of primary production and photoacclimation. *Applied Optics*, *59*(10), C100–C114. https://doi.org/10.1364/AO.386252

Shigesada, N., & Okubo, A. (1981). Analysis of the self-shading effect on algal vertical distribution in natural waters. *Journal of Mathematical Biology*, *12*(3), 311–326. https://doi.org/10.1007/BF00276919

Strogatz, S. H. (2015). *Nonlinear dynamics anc chaos: With applications to physics, biology, chemistry and engineering*. (2nd ed.). Westview Press. https://doi.org/10.1201/9780429492563

Sverdrup, H. U. (1953). On conditions for the vernal blooming of phytoplankton. *Journal du Conseil International pour l'Exploration de la Mer*, *18*(3), 287–295. https://doi.org/10.1093/icesjms/18.3.287

Weissing, F. J., & Huisman, J. (1994). Growth and competition in a light gradient. *Journal of Theoretical Biology*, *168*(3), 323–336. https://doi.org/10.1006/jtbi.1994.1113

Westberry, T. K., Silsbe, G. M., & Behrenfeld, M. J. (2023). Gross and net primary production in the global ocean: An ocean colorremote sensing perspective. *Earth-Science Reviews*, *237*, 104322. https://doi.org/10.1016/j.earscirev.2023.104322

Williams, R. G., & Follows, M. J. (2011). *Ocean dynamics and the carbon cycle*. (1st ed.). Cambridge University Press. https://doi.org/10.1017/CBO9780511623370